Journal of Applied Fluid Mechanics, Vol. 13, No. 3, pp. 815-826, 2020.
Available online at www.jafmonline.net, ISSN 1735-3572, EISSN 1735-3645.
DOI: 10.29252/jafm.13.03.30454

Mitigation of Flow Maldistribution in Minichannel and Minigap Heat Exchangers by Introducing Threshold in Manifolds

P. Dąbrowski

Gdańsk University of Technology, Gdańsk, Pomorskie, 80-233, Poland

†*Corresponding Author Email: pawel.dabrowski@pg.edu.pl*

(Received April 30, 2019; accepted September 17, 2019)

ABSTRACT

In the present paper, a detailed numerical investigation has been carried out to analyze the flow maldistribution in 50 parallel rectangular cross-section (1 mm depth and 1 mm width) minichannels and minigap section (1 mm depth and 99 mm width) with rectangular/trapezoidal manifolds in Z-type flow configuration. The author carried out numerical investigation with various mass flow rates, namely 0.05 kg/s, 0.1 kg/s and 0.2 kg/s which results in Reynolds number of 1532, 3064, 6128 respectively. A novel approach for the mitigation of non-uniform flow has been proposed introducing threshold at the entrance of the minigeometry section. The conventional case without threshold (as reference) and 1 mm, 3 mm and 7 mm threshold were introduced. The threshold has been employed by making a manifolds' depth bigger than section's depth. The maldistribution coefficient can be reduced twice in minigap section or three times in the minichannel section already with the 1 mm threshold as compared to the arrangement without threshold. It is found that rectangular manifold gives lower maldistribution coefficient than trapezoidal manifold which corresponds with actual state of the art. The distribution is more uniform in minichannel section than in minigap section for the same inlet parameters. To obtain uniform distribution of fluid flow should be stabilized already at the inlet manifold, at the entrance to the minichannel or minigap section. That was done by introducing the threshold in the manifolds, which is novelty of this study.

Keywords: Minigeometry; Flow distribution; Manifold shape; Manifold's depth; CFD; Numerical study.

NOMENCLATURE

d	manifold's depth	Re	Reynolds number
g	gravity acceleration	t	section's threshold
M	mass flow rate	T	temperature
N	number of channels, number of points	*V*	velocity vector
m	mean index		
n	normalized index	μ	dynamic viscosity
o	overall index	ρ	density
p	pressure	Φ	maldistribution coefficient

1. INTRODUCTION

Heat exchangers with minigeometries are becoming more and more popular. Initially, they were used to cool electronic devices (Tuckerman and Pease, 1981) but now there are a lot more of application where minichannels or minigaps can be found. There are among others: power industry (Mikielewicz & Mikielewicz, 2010), space industry (Brutin *et al.* 2013), automotive industry (Sakamatapan & Wongwises, 2014), avionics industry (Najim & Feddaoui, 2018), solar industry (Zhou *et al.* 2017), cryogenic industry (Zhou *et al.* 2014), refrigeration industry (García-Cascales *et al.* 2017), chemical and biological industry (Amador *et al.* 2004). There are also some works that are trying to combine the minichannels with nanofluids (Uysal *et al.* 2019).

Heat exchangers with minigeometries such as minichannels or minigaps seem to characterize by good thermal parameters such as heat transfer coefficient and good compactness. However, small diameter of minichannel causes a low mass flux of fluid that is able to flow through it and slight heat flux that can be dissipated from the cooled surface as a result. That is a reason for the application of many parallel minichannels with common inlet and outlet manifold. But this kind of construction causes a flow maldistribution. The flow maldistribution can be defined as a non-uniform or irregular flow of fluid in individual channels. It is an unfavorable phenomenon that can result in non-uniform temperature distribution along with the heat exchanger, presence of hot-spots and efficiency reduction. The maldistribution is not examined well enough and there are inconsistencies in reports about reasons, predictions and methods of reduction. Moreover, there are a lot of works that are dealing with a maldistribution phenomenon in parallel minichannels (Dąbrowski *et al.* 2019; García-Cascales *et al.* 2017; Kumar and Singh, 2019; Najim & Feddaoui, 2018; Dąbrowski *et al.* 2017; Sakamatapan & Wongwises, 2014; Yang *et al.* 2017; Zhou *et al.* 2014) but few that mentioned about flow non-uniformity and non-uniform temperature field in minigaps (Alam *et al.* 2013; Mathew *et al.* 2019; Tamanna & Lee, 2015).

A very significant part of designing heat exchangers is to choose the proper inlet and outlet manifold configuration. Numerical study where comparisons of some flow fields were made in (Mu *et al.* 2015), and it was determined that the bifurcation structure manifold gives excellent distribution, which resulted in a very uniform temperature field over the heating surface. The numerical optimization of the flow distribution on an inlet manifold was proposed by (Chien *et al.* 2019). Authors demonstrated an optimization model that reduces the flow maldistribution over 6.5 times compare to the case without an optimized manifold. The novel manifold configuration was examined by (Shao *et al.* 2018) in their numerical studies of double tube-passes shell and tube heat exchanger with a rectangular header. Two inlet tubes with several holes on the back were inserted into the inlet header to uniform the flow distribution of the first tube-pass. Similarly, two outlet tubes with several holes on the front were also inserted into the outlet header. This operation resulted in better distribution of fluid. The experimental investigation of manifold shape and configuration on flow maldistribution has been performed by (Anbumeenakshi & Thansekhar, 2016). It showed that vertical flow inlet configuration results in better fluid distribution than inline flow configuration. Authors claimed that flow maldistribution can be minimized with proper selection of the inlet configuration and header shape. A comprehensive study related to flow distribution in manifolds was summarized in (Wang, 2011). Here can be found theoretical models, analytical solutions and many comparisons concerning the role of the manifold in the flow distribution.

Many authors tried to found a good and universal solution for mitigating the flow maldistribution effect. Most of them are focused on geometrical modifications of channels or manifolds. Tuo and Hrnjak (2013) found out that the flow maldistribution is caused by the pressure drop in headers. To reduce uneven distribution the ratio of outlet header pressure drop to total evaporator pressure drop have to be reduced. They proposed the following solutions to significantly reduce maldistribution impact: enlarging the outlet header diameter, increasing heat exchanger's length to the width aspect ratio, or reducing the microchannel. The numerical study on mitigation of the flow maldistribution in parallel microchannels was done by (Kumar *et al.* 2018). Authors proposed a new concept of variable width channels. It is noticed that a new design mitigates maldistribution factor of the conventional design by 93.7%. Uniformity in flow distribution also brings uniformity in heat removal. The same authors have studied their approach more (Kumar *et al.* 2019) and carried out a new solution based on variable height microchannels. They compared their two approaches and found out that the variable height microchannel approach is more efficient than variable-width microchannel heat sink in the computation time-saving. Nevertheless, both approaches effectively improve distribution in channels. Another numerical simulation was done by (Tang *et al.* 2017) where authors proved that a significant flow maldistribution exists inside the Self-Similarity Heat Sink (SSHS). Modifications to the structure of SSHS, namely the inlet manifold channel and the inlet plenum were done. The tapered contracting structure was proposed to mitigate the maldistribution phenomenon. The novel inlet/outlet arrangement with various flow inlet angle was proposed by (Kumar & Singh, 2019). This flow maldistribution solution was analyzed numerically. It is found that flow distribution changes with flow inlet angle and minimum flow maldistribution are observed for the proposed angle of 105°. Better fluid distribution results in better and more uniform cooling of the heat sink. However, further increment in the flow inlet angle increases the non-uniformity.

It is clear that a lot of researchers are dealing with the problem of the flow maldistribution mitigation. They are modifying the geometry of inlet/outlet manifolds or minichannels, mainly changing their dimensions. The current paper discusses the novel method of mitigating the flow maldistribution phenomenon in minichannel and minigap heat exchangers introducing the threshold at the entrance to the minigeometry section. To the best of the author's knowledge, such a solution has not been discussed yet. Moreover, there are few investigations concentrated on non-uniformity in minigaps or which compare minigaps with minichannels (Alam *et al.* 2013; Mathew *et al.* 2019). Therefore, there is a need for in-depth study to take a closer look at fluid flow in minigap sections, to investigate the influence of manifolds' geometry on flow maldistribution and to compare minigaps with minichannels. In the present work, a detailed numerical investigation was carried out to

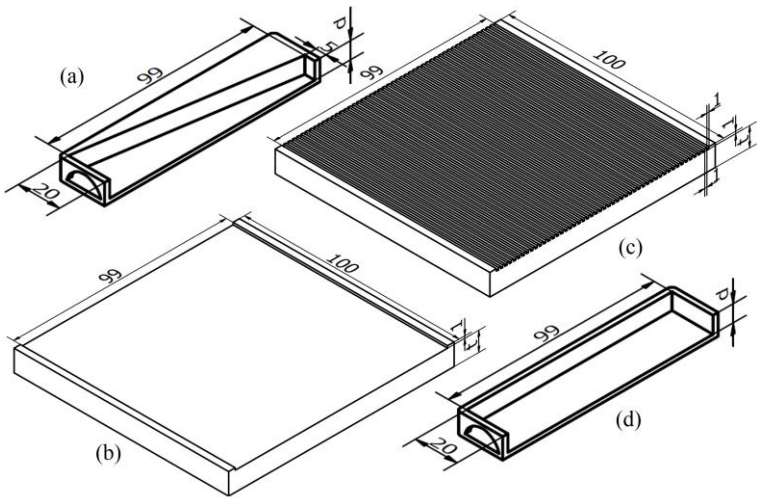

Fig. 1. Physical model of manifolds and sections used in the numerical simulation (a) trapezoidal manifold (b) minigap section (c) minichannel section (d) rectangular manifold.

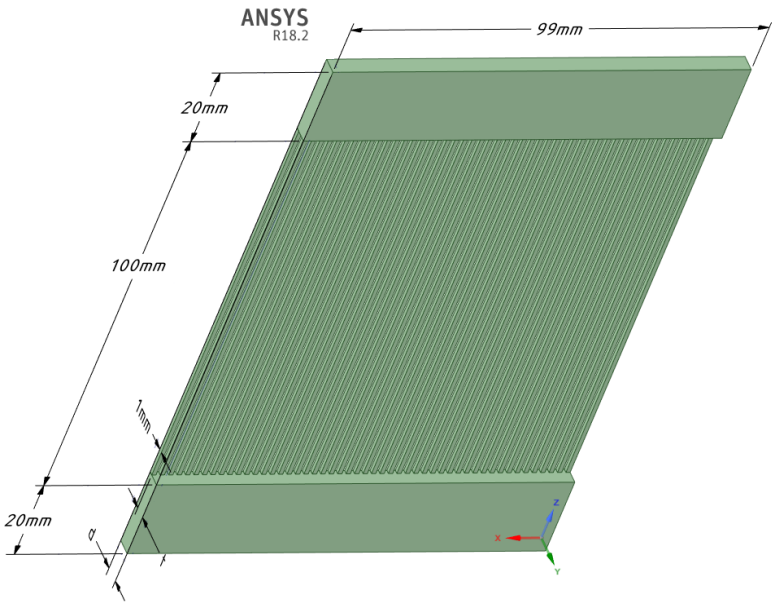

Fig. 2. Fluid domain of minichannel section with rectangular manifolds.

examine the effect of manifolds' depth (threshold) on flow distribution through the minigap and minichannel sections.

2. CFD MODEL DETAILS

A three-dimensional model of the heat exchangers with various inlet and outlet manifolds were created with the Autodesk Inventor software. Then, models were exported to the ANSYS SpaceClaim software to prepare the fluid domains. The fluid flows in the opposite direction to the Z and X axes.

2.1 Physical Model

Two sections to which fluid was flowing, namely minigap and minichannel section in Z-type flow configuration were taken into account. All the significant dimensions were shown in Fig. 1. Minichannel section consisted of 50 rectangular channels with 1 mm fin spacing. The depths of channels and minigap were 1 mm in all cases. In the calculations, sections were connected with inlet and outlet manifold with various shapes, namely rectangular and trapezoidal. Various depths d of the manifolds results in a various threshold t (always 1 mm smaller than depth) at the interface between the section and the manifold. All the dimensions of the sections were summarized in Table 1.

The examples of the fluid domains that were taken into account are shown in Fig. 2 and Fig. 3. Figure 2 shows the minichannel section with rectangular manifolds and Fig. 3 shows the minigap section with trapezoidal manifolds but there were much more cases. The minichannel and minigap sections were connected with rectangular and trapezoidal manifolds as well. Each section has the manifolds with the whole spectrum of depths,

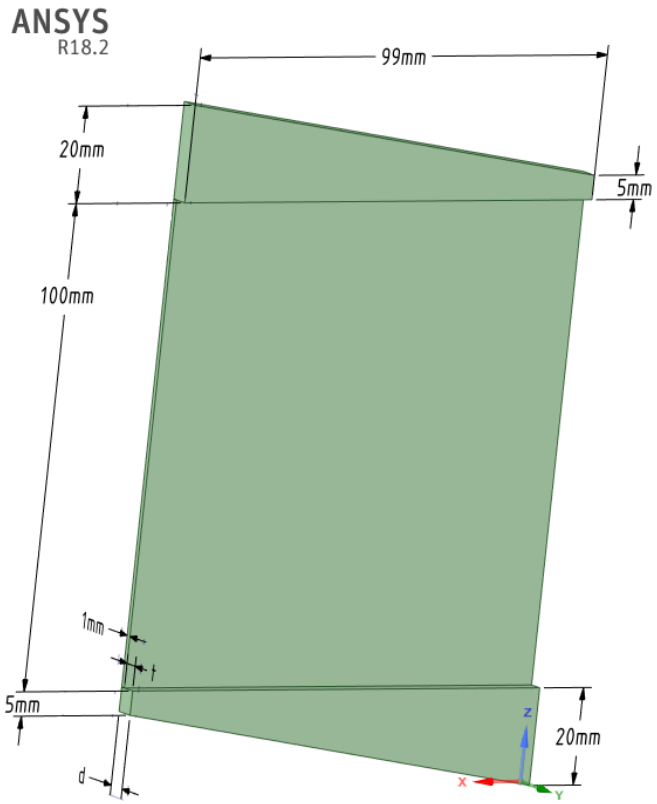

Fig. 3. Fluid domain of minigap section with trapezoidal manifolds.

namely from 1 mm to 8 mm, which results in thresholds from 0 mm (no threshold/conventional case) to 7 mm. All the dimensions of the manifolds were summarized in Table 2.

Table 1 Geometrical parameters of the sections

Section			
Minichannel		Minigap	
Parameter	Value	Parameter	Value
Depth	1 mm	Depth	1 mm
Width	1 mm	Width	99 mm
Fin spacing	1 mm	Hydraulic diameter	1.98 mm
Hydraulic diameter	1 mm		
Number of channels	50		

Table 2 Geometrical parameters of the manifolds

Manifold			
Trapezoidal		Rectangular	
Parameter	Value	Parameter	Value
Depth	1÷8 mm	Depth	1÷8 mm
Width	20/5 mm	Width	20 mm
Threshold	0÷7 mm	Threshold	0÷7 mm

2.2 Governing Equations

To investigate the effect of changing depth (and threshold as well) of the inlet and outlet manifold on flow maldistribution of minichannel and minigap heat exchangers the following assumptions were taken:

- Fluid flow is a single-phase, in steady-state, incompressible and three dimensional.
- Properties of fluid are independent of temperature and pressure.

According to above-mentioned assumptions, the governing equations for the fluid domain are continuity and momentum equations (Eq. (1) and Eq. (2)).

$$\nabla \cdot \vec{V} = 0 \tag{1}$$

$$\rho(\vec{V} \cdot \nabla \vec{V}) = -\nabla p + \mu \nabla^2 V \tag{2}$$

The gravity acceleration g=9.81 m/s^2 is consistent with the direction of the Y-axis.

In FLUENT 18.2 the conservation equations of mass and momentum are solved using finite volume method (FVM). There are several turbulence models available. In this case, the model SST k-omega has been chosen. A segregated implicit solver with Coupled pressure correction algorithm has been chosen to compute the velocity field in manifolds and minigap or minichannel section. Momentum equations are discretized by second-order upwind scheme.

2.3 Boundary Conditions

For all the considered cases, water was chosen as a working fluid. The inlet parameters for water

are $\rho = 992.2$ kg/m^3, $\mu = 6.53 \times 10^{-4}$ Pa*s, T=313.15 K and p=100 kPa. The flow was assumed as an adiabatic. The mass flow rate M at the inlet to the heat exchanger was varied from 0.05 to 0.2 kg/s. The outlet of the heat exchanger was assumed as a pressure outlet. The mean Reynolds number Re_m in a single minichannel and minigap was varied from 1532 to 6128 and the mean velocity V_m from 0.5 to 4 m/s. When the residual values become less than 10^{-6} for the continuity, x-velocity, y-velocity, and z-velocity, the solutions are considered to be converged. The summary of geometrical and hydrodynamic parameters in all investigated cases was shown in Table 3.

Table 3 Boundary conditions and hydrodynamic parameters in all investigated cases

			Minichannel section		Gap section	
M	d	t	V_m	Re_m	V_m	Re_m
0.05 kg/s	1	0	1 m/s	1532	0.5 m/s	1532
	2	1				
	4	3				
	8	7				
0.1 kg/s	1	0	2 m/s	3064	1 m/s	3064
	2	1				
	4	3				
	8	7				
0.2 kg/s	1	0	4 m/s	6128	2 m/s	6128
	2	1				
	4	3				
	8	7				

3. MODEL VALIDATION

The normalized velocity V_n was used to show the independence of the grid. The normalized velocity is a ratio of the actual velocity at the considered point of the section to the mean velocity, which should be if the flow was uniform. The mathematical expression of normalized velocity is shown in Eq. (3).

$$V_{n,i} = \frac{V_i}{V_m} \tag{3}$$

Fluid domain was discretized using ANSYS Fluent with tetrahedral control volumes in manifolds and hexahedral control volumes in channels. Computational cells with 5.6×10^6, 6.2×10^6 and 6.6×10^6 elements were taken into consideration to test the grid independence of the solution. In Fig. 4, the normalized velocity distribution in the 50 channels in the 4 mm depth rectangular manifold and mass flow rate of 0.1 kg/s is shown. It is observed that all cases have almost the same normalized velocity distribution in parallel minichannels. The grid parameters that give 6.2×10^6 elements was chosen for all the simulation cases.

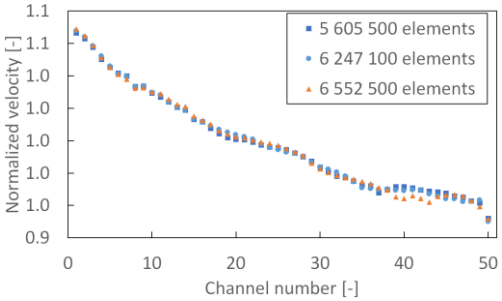

Fig. 4. Grid independence.

4. RESULTS AND DISCUSSION

The minigap and minichannel section with rectangular or trapezoidal manifold (depth 1 ÷ 8 mm) and mass flow rate of 0.05 ÷ 0.2 kg/s cases were analyzed. It results in 24 cases (12 for minichannel section and 12 for minigap section). For every single case, the flow velocity profile was obtained. Then, the flow maldistribution coefficient in i-th of 50 channels in minichannel section or in i-th of 50 points over the width of the minigap section was calculated from Eq. (4).

$$\Phi_i = \sqrt{\left(\frac{M_i - M_m}{M_m}\right)^2} \tag{4}$$

The overall maldistribution coefficient in every case was calculated as a standard deviation of N=50 previously calculated points (Eq. (5))

$$\Phi_o = \frac{\sum_{i=1}^{N} \Phi_i}{\sqrt{N}} = \sqrt{\frac{1}{N}\sum_{i=1}^{N}\left(\frac{M_i - M_m}{M_m}\right)^2} \tag{5}$$

4.1 Minigap

The XZ plane velocity profile at the center (0.5 mm from the bottom wall) of the minigap is shown in Fig. 5. With the increase of the manifolds' depths, the flow uniformity increases. Moreover, there are fewer spots where the velocity is close to 0 m/s. When the manifold's depth is equal to the minigap section's depth (no threshold), there is no possibility for flow to get uniformed before entering the section. Fluid flows mainly diagonally from inlet to outlet, causing big space on the section where the velocity is near 0 m/s. The flow maldistribution is high because of the possibility to flow in two-dimensions; parallel and perpendicular to the minigap section. Increasing the depth provides a threshold before the section, where the flow is stabilizing, being more uniform and starting to flow mainly parallel to the minigap section. Already at the depth of 2 mm (the threshold equal to 1 mm), about 85% of section's area is active, in comparison to about 60% of the active area without threshold.

The isometric view of a rectangular inlet manifold of the minigap section with streamlines colored by velocity is shown in Fig. 6. With increasing the manifold's depth streamlines enter the minigap section more parallel, reducing the effect of two-dimensional flow. The flow is stabilizing in a

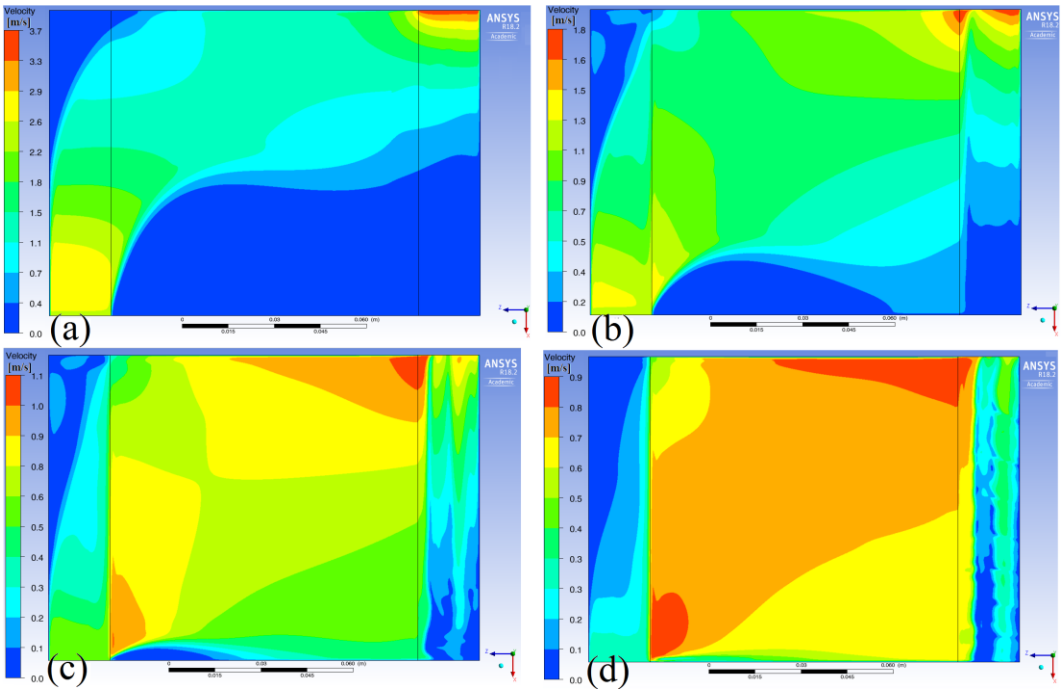

Fig. 5. Velocity profile in a minigap section with rectangular manifold for various manifolds' depths and mass flow rate of 0.05 kg/s (a) depth of 1 mm (b) depth of 2 mm (c) depth of 4 mm (d) depth of 8 mm.

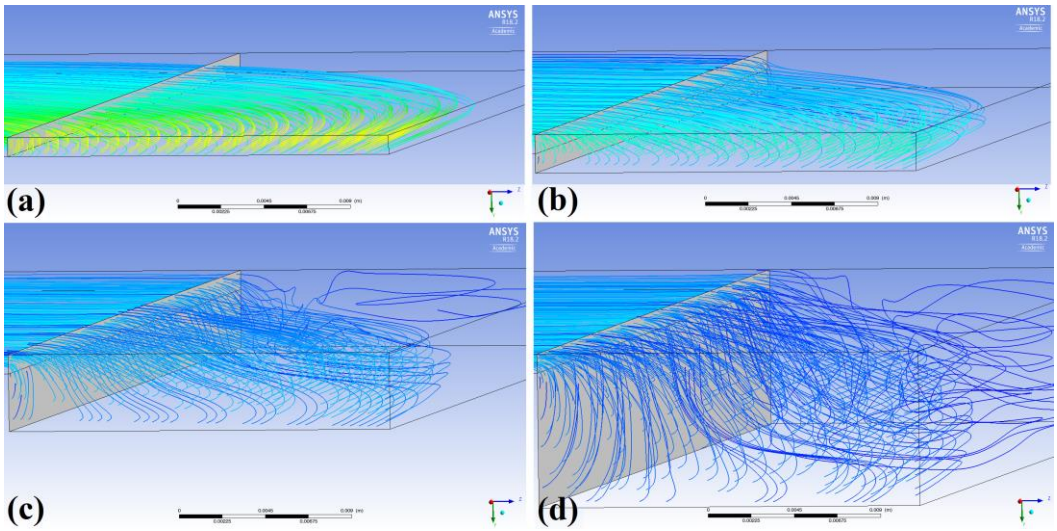

Fig. 6. Streamlines in the inlet rectangular manifold of the minigap section for various manifold's depths and mass flow rate of 0.05 kg/s (a) depth of 1 mm (b) depth of 2 mm (c) depth of 4 mm (d) depth of 8 mm.

manifold and enters the minigap section over the whole width. However, there are some vortexes and backflows in a manifold, away from the inlet intensifying with manifold's depth increasing.

Similar isometric view as in Fig. 6 is shown in Fig. 7 but for the outlet manifold. The streamlines in a view (d) are parallel. They leave the minigap section, falling down into the outlet manifold, creating two characteristic vortexes.

Figure 8 shows the curve of a maldistribution coefficient in a minigap with varying depth of the manifolds for various mass flow rates. The overall maldistribution coefficient in a whole section is decreasing with the increase of the manifold's depth. Irrespective of the manifold type (rectangular or trapezoidal) the biggest relative decrease of maldistribution coefficient is already at the small manifold's depth. This relationship seems to be a rational function. The maldistribution coefficient can be reduced nearly twice by increasing the depth by 1 mm (introducing the threshold of 1 mm). Already at a depth of 4 mm, further increasing the manifold's depth does not bring much effect. The fluid flow over the minigap is quite well distributed. Moreover, worse distribution is manifested at

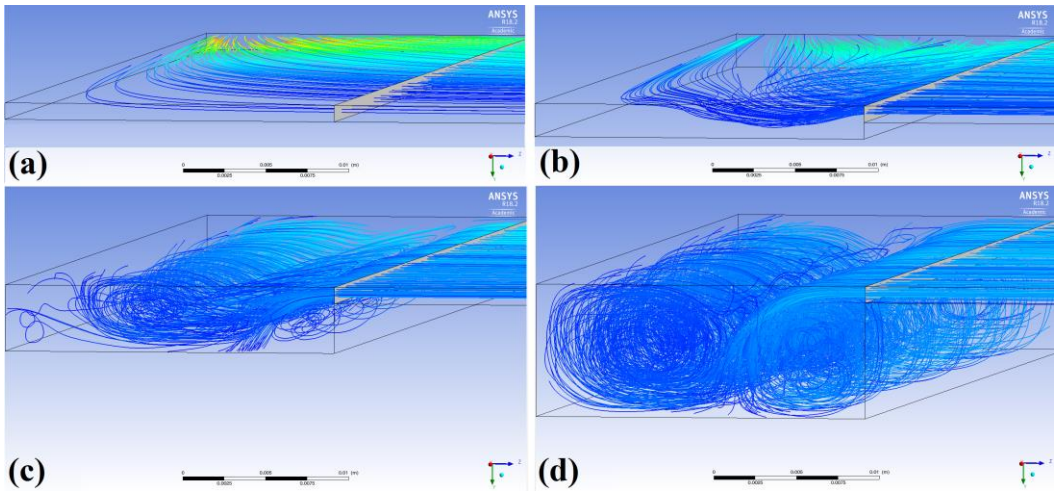

Fig. 7. Streamlines in the outlet rectangular manifold of the minigap section for various manifold's depths and mass flow rate of 0.05 kg/s (a) depth of 1 mm (b) depth of 2 mm (c) depth of 4 mm (d) depth of 8 mm.

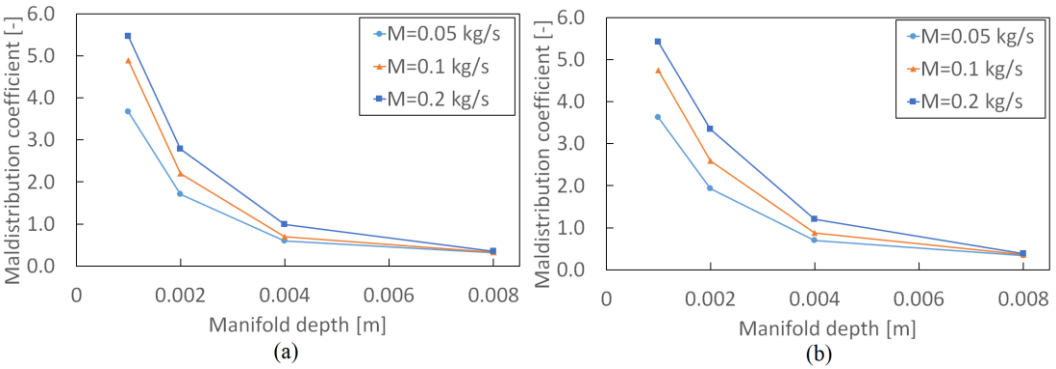

Fig. 8. Maldistribution coefficient for various manifolds' depths in a minigap for different mass flow rates (a) rectangular manifold (b) trapezoidal manifold.

higher flow rates. Slightly higher maldistribution can be observed in the case of a trapezoidal manifold in comparison with a rectangular manifold, which corresponds with findings from (Anbumeenakshi & Thansekhar, 2016; Kumaraguruparan *et al.* 2011).

The distribution of a maldistribution coefficient along the minigap is shown in Fig. 9. As said before the higher mass flow rate the worsen distribution of fluid along the minigap. Moreover, the point at which the lowest maldistribution can be observed is shifted towards the inlet as the mass flow rate increases. For a mass flow rate of 0.05 kg/s, the lowest maldistribution is located at 52 mm from the inlet whereas for a mass flow rate of 0.2 kg/s at 40 mm from the inlet. It is also shown that severe maldistribution (maldistribution coefficient up to 1.6) is always towards the inlet form the lowest maldistribution point while better distribution (maldistribution coefficient up to 0.9) can be observed further from the inlet, after the characteristic point.

It is worth to mention that introducing the threshold in a minigap section complicates the exchanger's design and increases its overall dimensions. Using this solution, greater focus is required on designing the appropriate inlet to the heat exchanger as well as the outlet. In addition, increasing the depth of manifolds compared to minigap's depth results in more complex mechanical machining of the heat exchanger during manufacture. However, the benefits of maldistribution reduction are unquestionable.

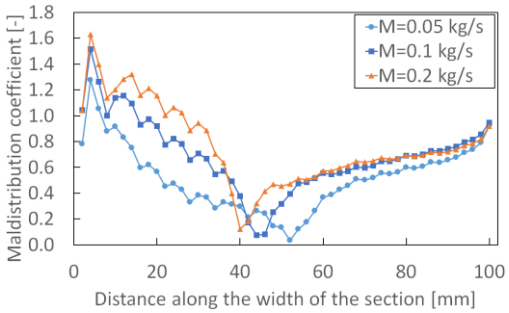

Fig. 9. Maldistribution coefficient along the minigap width with 1 mm depth rectangular manifold for various mass flow rates.

4.2 Minichannels

The XZ plane velocity profile at the center (0.5 mm

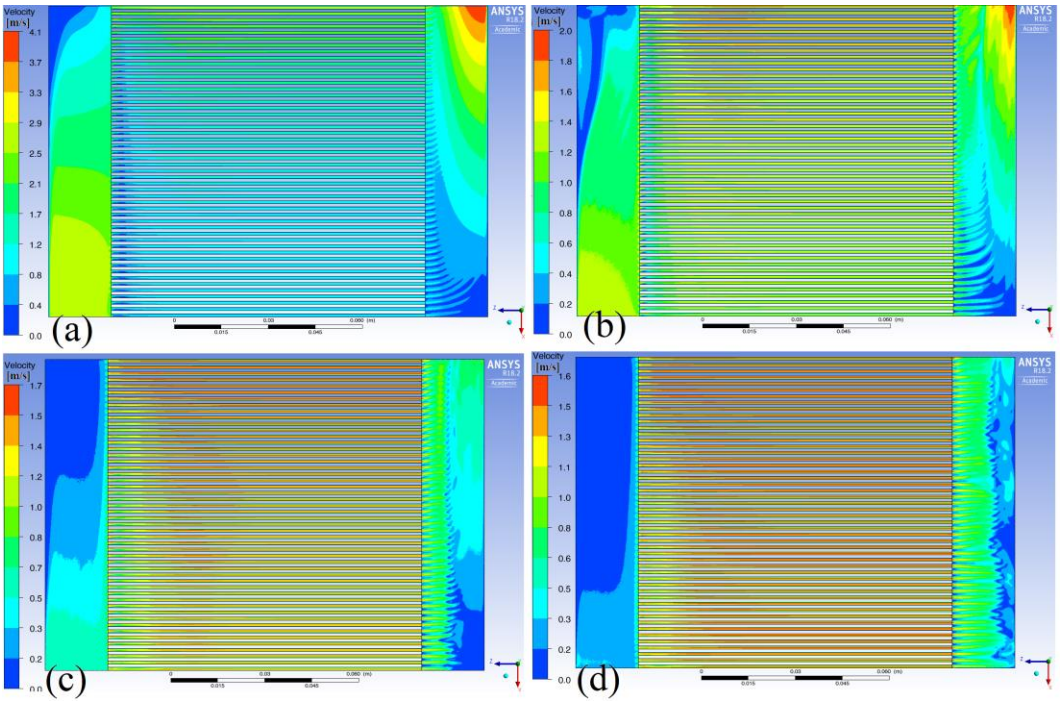

Fig. 10. Velocity profile in minichannels section with rectangular manifold for various manifolds' depths and mass flow rate of 0.05 kg/s (a) depth of 1 mm (b) depth of 2 mm (c) depth of 4 mm (d) depth of 8 mm.

from the bottom wall) of the minichannels is shown in Fig. 10. It is seen that quite uniform flow is obtained already at the depth of 2 mm which is 1 mm under the minichannels bottom wall. This 1 mm high threshold before the minichannel section provides the possibility to stabilize flow and distribute fluid to every channel equally. With the increase of the inlet manifold's depth, the fluid velocity in the whole collector decreases in the center XZ plane of the channels. Only near to the channels' entrance, there is a local increase in the velocity. This testifies the way of fluid distribution, which, by filling the large space of the collector, stabilizes and distributes evenly to the channels.

Figure 11 gives a better view of the fluid distribution in the inlet manifold of a minichannel section. The threshold that is formed by increasing the manifold's depth causes that the liquid which flows to the heat exchanger does not immediately enters the minichannel section but first stabilizes in the inlet manifold. Due to this phenomenon, the flow is more uniform over the section's width. Chien *et al.* (2019) have also obtained lower maldistribution coefficients by modifying inlet manifold in their numerical optimization work.

The streamlines distribution in outlet rectangular manifold of the minichannel section is shown in Fig. 12. The bigger the depth of manifold, the more vortexes in the outlet manifold. The fluid after exiting the minichannels section is filling the manifold first and then flows to the outlet of the heat exchanger. The threshold created by the difference between manifold's and minichannel section's depth behaves as a sort of "waterfall" making the flow more turbulent and chaotic.

The effect of manifold's depth on maldistribution reduction in minichannels is significant. The maldistribution coefficient and manifold's depth relationship is shown in Fig. 13. The maldistribution coefficient can be reduced over three times by increasing the depth by 1 mm (introducing 1 mm threshold). Continuous increase twice the depth of the collector causes a relative decrease in the maldistribution coefficient of more than three times, but the absolute reduction after the depth of 2 mm is not so high. The differences between trapezoidal and rectangular manifolds are also not significant with a slight improvement in distribution to a rectangular one.

The maldistribution coefficient in every single channel is shown in Fig. 14. The channel at which the lowest maldistribution can be observed is the same regardless of the mass flow rate. The maldistribution in channels preceding the lowest maldistribution channel (closer to the inlet) is severe (maldistribution coefficient up to 1.2) while after the 20th channel, the character of maldistribution has changed. The maldistribution coefficient is rising in channels that are further away from inlet but still the maximum coefficient is not as high as mentioned before (just up to 0.6).

4.3 Comparisons

As can be seen from the above considerations, the flow maldistribution in minigaps and minichannels differs from each other. There are some general

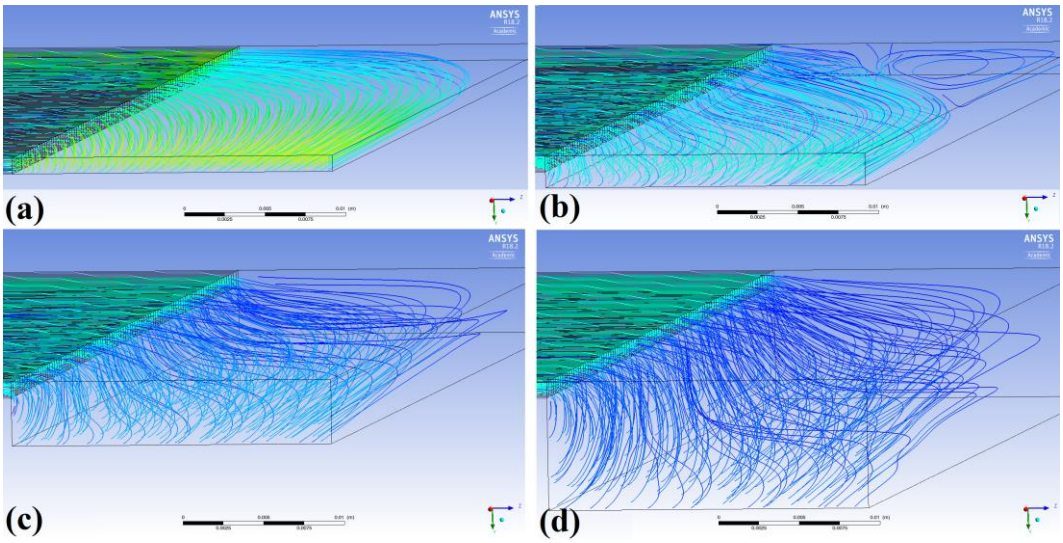

Fig. 11. Streamlines in the inlet rectangular manifold of the minichannel section for various manifold's depths and mass flow rate of 0.05 kg/s (a) depth of 1 mm (b) depth of 2 mm (c) depth of 4 mm (d) depth of 8 mm.

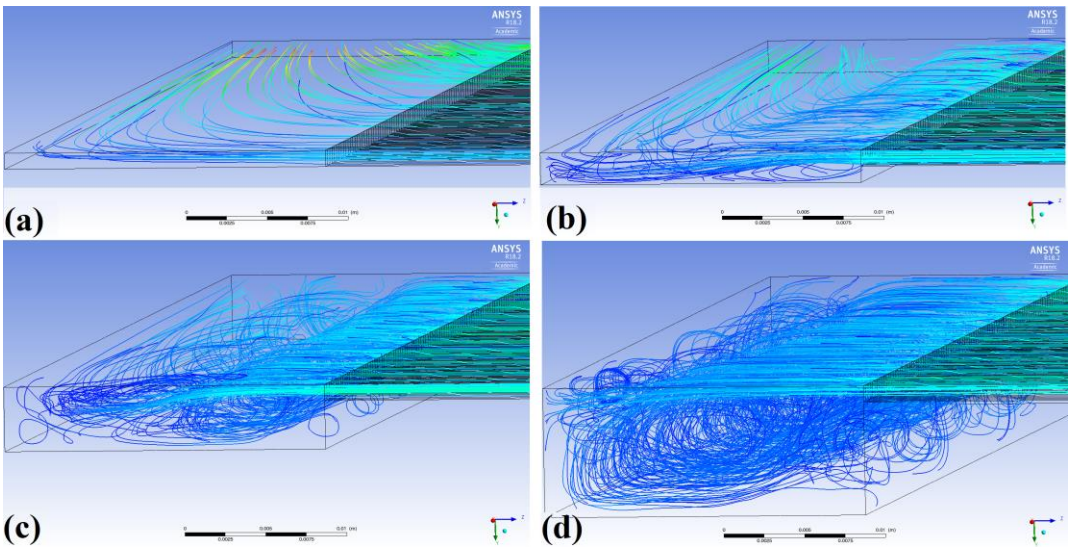

Fig. 12. Streamlines in outlet rectangular manifold of the minichannel section for various manifold's depths and mass flow rate of 0.05 kg/s (a) depth of 1 mm (b) depth of 2 mm (c) depth of 4 mm (d) depth of 8 mm.

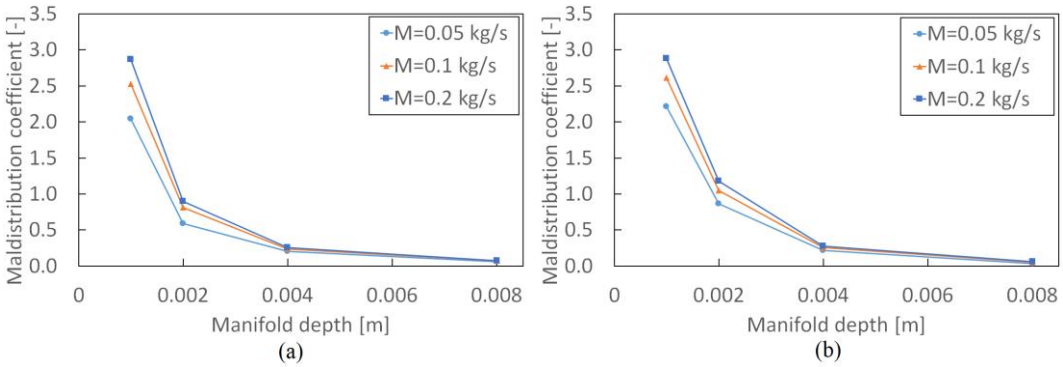

Fig. 13. Maldistribution coefficient for various manifolds' depths in minichannels for different mass flow rates (a) rectangular manifold (b) trapezoidal manifold.

similarities in the qualitative point of view but both geometries differ in a quantitative point of view. Fig. 15 shows the comparison of the maldistribution coefficient for various manifolds' depths in a minigap and minichannels for maximum and minimum of considered mass flow rates. The distribution in channels is from 2 to 3 times better than in minigap for every case. Nevertheless, the curves have the same character and the biggest reduction of the maldistribution coefficient can be obtained increasing the depth of manifolds from 1 mm to 2 mm (introducing 1 mm threshold).

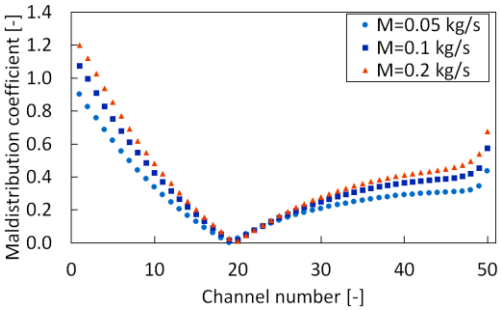

Fig. 14. Maldistribution coefficient in every channel with 1 mm depth rectangular manifold for various mass flow rates.

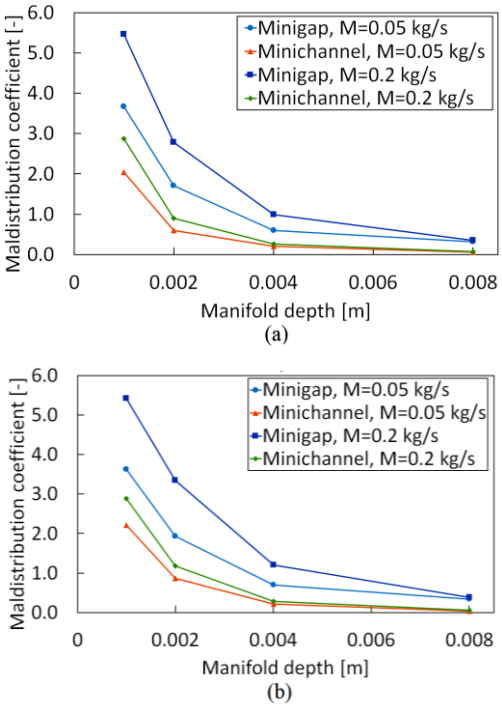

Fig. 15. Maldistribution coefficient for various manifolds' depths in a minigap and minichannels for different mass flow rates (a) rectangular manifold (b) trapezoidal manifold.

The comparison of manifolds geometry, namely trapezoidal and rectangular manifold both for minigap and minichannels section is shown in Fig. 16. The distribution in a section, provided with the rectangular as well as the trapezoidal manifold is not visibly differed when the depth of the manifolds are at the same level as the minigap or minichannels (there is no threshold). The difference appears at bigger depths and then trapezoidal manifold results in slightly higher (about 20%) maldistribution coefficient than the rectangular manifold. It is so in minichannels as well as in minigap.

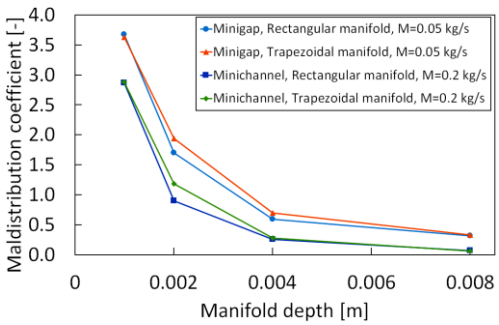

Fig. 16. Maldistribution coefficient for various manifolds and their depths in a minigap and minichannels for different mass flow rates.

The normalized velocity distribution in the minigap and minichannel section differs from each other. The velocity field in minichannels is more uniform, stable and less chaotic than across the minigap section. It is shown in Fig. 17. It is so due to the fact that flow in channels is one-dimensional. The fluid flows only along channels. The velocity field in the minigap section is more complex. The fluid is able to flow along gap as well as across gap. This flow is more like two-dimensional. Anyway, there are no significant differences between minigap and minichannels section's fluid distribution at the higher depths excluding sudden fall of normalized velocity at the left (0 mm) and right (100 mm) end of the section. This fall is caused by wall effects (hydrodynamic boundary layer). The same effect is not present in the minichannels, because every channel is separated geometry with their own walls.

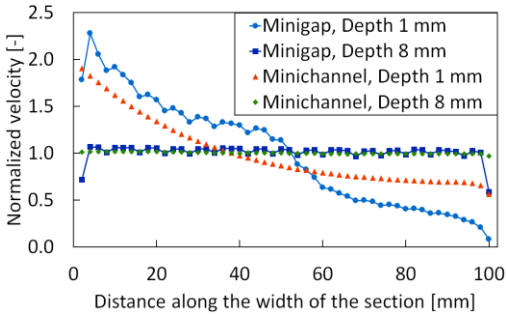

Fig. 17. Normalized velocity profile in a minigap and minichannels for various rectangular manifolds' depths for a mass flow rate of 0.05 kg/s.

The comparison of a maldistribution coefficient along the width of the minichannels and minigap section is shown in Fig. 18. It is seen that increasing the depth gives better results in minichannels section than the minigap section. Moreover, the point where the actual velocity is equal to uniform velocity is closer to the inlet in minichannels (about

40 mm from the inlet, which is 20th channel) than in minigap section (about 50 mm from inlet).

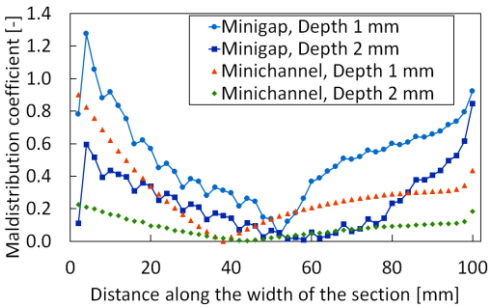

Fig. 18. Maldistribution coefficient along a section width in a minigap and minichannels for various rectangular manifolds' depths for a mass flow rate of 0.05 kg/s.

5. CONCLUSIONS

A detailed numerical investigation was performed to reduce the flow maldistribution in minichannel and minigap heat exchangers using a novel manifold threshold approach. A minigeometries sections fed by manifolds without threshold (conventional) and with threshold has been considered and fluid domain simulation was carried out. Based on the above results, the following conclusions were made.

1. Introduction of the threshold between inlet/outlet manifold and section results in better distribution of fluid. The flow in 50 parallel channels and minigap as well has been more uniform. The maldistribution coefficient can be reduced twice in minigap section or three times in the minichannel section already with the 2 mm depth manifolds as compared to the arrangement without threshold.
2. It is observed that the use of rectangular manifold results in better distribution than the trapezoidal manifold, which corresponds with findings from (Anbumeenakshi and Thansekhar, 2016). Moreover, lower maldistribution coefficient was obtained for lower mass flow rates, which is known from (Kumaraguruparan *et al.* 2011).
3. More uniform distribution can be observed in the minichannel section than in the minigap section. Introduction of the threshold reduces flow maldistribution in both sections. However, the minichannel section shows slightly better maldistribution mitigation characteristic in the function of the manifolds' depth than minigap section.
4. The minigap section suffers more from non-uniform distribution of fluid due to two-dimensional flow over a minigap in comparison to one-dimensional flow in a channel. The flow maldistribution in minigap should be considered as a maldistribution field over the whole surface rather than the one-dimensional approach as in a minichannel section.
5. The results presented in this paper demonstrate that special attention should be given to the design of the manifold, in order to reduce flow maldistribution. Similar conclusions were made by (Anbumeenakshi and Thansekhar, 2016; Tang *et al.* 2017; Kumar and Singh, 2019). Good and stabilized distribution of fluid should be assured already in the inlet manifold.

ACKNOWLEDGEMENTS

The work presented in this paper was funded from the National Science Centre, Poland research project No. 2017/27/N/ST8/02785 in the years 2018-2020.

REFERENCES

Alam, T., P. S. Lee, C. R. Yap and L. Jin (2013). A comparative study of flow boiling heat transfer and pressure drop characteristics in microgap and microchannel heat sink and an evaluation of microgap heat sink for hotspot mitigation. *International Journal of Heat and Mass Transfer* 58(1–2), 335–347.

Amador, C., A. Gavriilidis and P. Angeli (2004). Flow distribution in different microreactor scale-out geometries and the effect of manufacturing tolerances and channel blockage. *Chemical Engineering Journal* 101(1–3), 379–390.

Anbumeenakshi, C. and M. R. Thansekhar (2016). Experimental investigation of header shape and inlet configuration on flow maldistribution in microchannel. *Experimental Thermal and Fluid Science* 75, 156–161.

Brutin, D., V. S. Ajaev and L. Tadrist (2013). Pressure drop and void fraction during flow boiling in rectangular minichannels in weightlessness. *Applied Thermal Engineering* 51(1–2), 1317–1327.

Chien, N. B., N. X. Linh and O. Jong-Taek (2019). Numerical Optimization of Flow Distribution inside Inlet Header of Heat Exchanger. *Energy Procedia* 158, 5488–5493.

Dąbrowski, P., M. Klugmann and D. Mikielewicz (2017). Selected studies of flow maldistribution in a minichannel plate heat exchanger. *Archives of Thermodynamics* 38(3), 135–148.

Dąbrowski, P., M. Klugmann and D. Mikielewicz (2019). Channel Blockage and Flow Maldistribution during Unsteady Flow in a Model Microchannel Plate heat Exchanger. *Journal of Applied Fluid Mechanics* 12(4), 1023–1035.

García-Cascales, J. R., F. Illán-Gómez, F. Hidalgo-Mompeán, F. A. Ramírez-Rivera and M. A. Ramírez-Basalo (2017). Performance comparison of an air/water heat pump using a minichannel coil as evaporator in replacement of a fin-and-tube heat exchanger. *International*

Journal of Refrigeration 74, 558–573.

Kumar, R., G. Singh and D. Mikielewicz (2018). A New Approach for the Mitigating of Flow Maldistribution in Parallel Microchannel Heat Sink. *Journal of Heat Transfer* 140(7), 72401–72410.

Kumar, R., G. Singh and D. Mikielewicz (2019). Numerical Study on Mitigation of Flow Maldistribution in Parallel Microchannel Heat Sink: Channels Variable Width Versus Variable Height Approach. *Journal of Electronic Packaging* 141(2), 21009–21011.

Kumar, S. and P. K. Singh (2019). Effects of flow inlet angle on flow maldistribution and thermal performance of water cooled mini-channel heat sink. *International Journal of Thermal Sciences* 138(February 2018), 504–511.

Kumaraguruparan, G., R. M. Kumaran, T. Sornakumar and T. Sundararajan (2011). A numerical and experimental investigation of flow maldistribution in a micro-channel heat sink. *International Communications in Heat and Mass Transfer* 38(10), 1349–1353.

Mathew, J., P. S. Lee, T. Wu and C. R. Yap (2019). Experimental study of flow boiling in a hybrid microchannel-microgap heat sink. *International Journal of Heat and Mass Transfer* 135, 1167–1191.

Mikielewicz, D. and J. Mikielewicz (2010). A thermodynamic criterion for selection of working fluid for subcritical and supercritical domestic micro CHP. *Applied Thermal Engineering* 30(16), 2357–2362.

Mu, Y. T., L. Chen, Y. L. He and W. Q. Tao (2015). Numerical study on temperature uniformity in a novel mini-channel heat sink with different flow field configurations. *International Journal of Heat and Mass Transfer* 85, 147–157.

Najim, M. and M. B. Feddaoui (2018). New cooling approach using successive evaporation and condensation of a liquid film inside a vertical mini-channel. *International Journal of Heat and Mass Transfe*r 122, 895–912.

Sakamatapan, K. and S. Wongwises (2014). Pressure drop during condensation of R134a flowing inside a multiport minichannel. *International Journal of Heat and Mass Transfer* 75, 31–39.

Shao, H., M. Zhang, Q. Zhao, Y. Wang and Z. Liang (2018). Study of improvements on fl ow maldistribution of double tube-passes shell-and-tube heat exchanger with rectangular header. *Applied Thermal Engineering* 144(January), 106–116.

Tamanna, A. and P. S. Lee (2015). Flow boiling heat transfer and pressure drop characteristics in expanding silicon microgap heat sink. *International Journal of Heat and Mass Transfer* 82, 1–15.

Tang, W., L. Sun, H. Liu, G. Xie, Z. Mo and J. Tang (2017). Improvement of flow distribution and heat transfer performance of a self-similarity heat sink with a modification to its structure. *Applied Thermal Engineering* 121, 163–171.

Tuckerman, D. B. and R. F. W. Pease (1981). High-performance heat sinking for VLSI. *IEEE Electron Device Letters* 2(5), 126–129.

Tuo, H. and P. Hrnjak (2013). Effect of the header pressure drop induced flow maldistribution on the microchannel evaporator performance. *International Journal of Refrigeration* 36(8), 2176–2186.

Uysal, C., E. Gedik and A. J. Chamkha (2019). A numerical analysis of laminar forced convection and entropy generation of a diamond-Fe 3 O 4 /water hybrid nanofluid in a rectangular minichannel. *Journal of Applied Fluid Mechanics* 12(2), 391–402.

Wang, J. (2011). Theory of flow distribution in manifolds. *Chemical Engineering Journal* 168(3), 1331–1345.

Yang, H., J. Wen, X. Gu, Y. Liu, S. Wang, W. Cai and Y. Li (2017). A mathematical model for flow maldistribution study in a parallel plate-fin heat exchanger. *Applied Thermal Engineering* 121, 462–472.

Zhou, J., X. Zhao, X. Ma, Z. Du, Y. Fan, Y. Cheng and X. Zhang (2017). Clear-days operational performance of a hybrid experimental space heating system employing the novel mini-channel solar thermal & PV/T panels and a heat pump. *Solar Energy* 155, 464–477.

Zhou, W., W. Deng, L. Lu, J. Zhang, L. Qin, S. Ma and Y. Tang (2014). Laser micro-milling of microchannel on copper sheet as catalyst support used in microreactor for hydrogen production. *International Journal of Hydrogen Energy* 39(10), 4884–4894.